

Transformations in Crystalline Ammonium Nickel Tutton Salt Induced by Infrared Hole Burning

Yun-Hwan Cha and Herbert L. Strauss*

Department of Chemistry, University of California, Berkeley, California 94720-1460

Received: May 24, 2000; In Final Form: July 20, 2000

The title compound doped with a small amount of deuterium shows infrared bands due to the N–D and O–D stretching vibrations. When one of the N–D bands is irradiated with an infrared laser, holes and anti-holes are produced. The pattern of these holes/anti-holes depends on the irradiation time. A ten-minute irradiation produces holes/anti-holes in the N–D bands only. A ten-second irradiation produces holes/anti-holes in the O–D bands as well. The features produced by the ten-second irradiation decay during the longer irradiation. Thus, the burning and decay kinetics of the Tutton salts involve processes that occur on at least two time scales.

The ammonium Tutton salts, $(\text{NH}_4)_2\text{X}(\text{H}_2\text{O})_6(\text{SO}_4)_2$, with X a divalent transition metal ion, form a series of well-known isomorphous crystals.¹ Introducing a small amount of deuterium produces crystals containing some NH_3D^+ ions and some HOD molecules. The Tutton salts all crystallize in the monoclinic space group $P2_1/a$ (#14) with the transition metal ion at a center of inversion. This ion is surrounded by the six water molecules in a distorted octahedron. The hydrogen atoms are equivalent in pairs: thus there are six distinct sets of H-atom sites. The water molecules are hydrogen bonded to the sulfate ions and these, in turn, to the ammonium ions. The ammonium ions sit in general sites, and so there are 4 distinct H positions for the ammonium hydrogen atoms.

The deuterium-doped crystals show a series of 10 distinct O–D and N–D bands, one for each distinct H (D) site. The different orientations of the HOD and NH_3D^+ molecules have slightly different energies since they put the D-atom in different inequivalent sites. The small energy differences determine the equilibrium distribution of the orientations at a given temperature.^{2,3}

We disturb the orientational distribution by irradiating the band corresponding to a given N–D band and then watch the relaxation back to equilibrium in the dark. We have previously reported on the effect of using a hole-burning laser for a period of about 30 min on a variety of ammonium Tutton salts—cobalt,² nickel, and their mixed crystals,^{4,5} and copper.⁶

For the copper salt, we noticed that the relaxation depended strongly on the time—that is, the relaxation was not a merely monotonic decay, but instead a result of a number of conformational processes occurring on different time scales.

Consequently, we developed an irradiation-spectrometer system to examine the kinetics on the order of seconds as well as over longer intervals. In this paper, we briefly explain the new apparatus and then consider the results of irradiating the ammonium nickel Tutton salt for two different periods, 10 s and 10 min. To compare results on such different time scales using a fixed power laser it is necessary to repeat the short irradiation process and its decay many times and co-add the results, and we do just that.

For the Cu salt and, to a lesser extent the Co salt, the Jahn–Teller effect produces a distorted octahedron of water molecules,

and this distortion can occur in two or three forms. For the Cu salt, this leads to the existence of at least two distinct crystals.⁷ No such effect is expected for the Ni salt, since Ni is an ion with no orbital degeneracy ($3d^8$: t_{2g}^6 , e_g^2).⁸ Nonetheless, markedly different results are observed for the two irradiation times.

Experimental Section

The experimental apparatus consists of a Nicolet 850 FTIR spectrometer with its associated computer and a difference-frequency laser system and associated optics.⁵ A counter timer (Keithly Instruments CTM-05/A) was added to the PC computer. The counter timer controls the relationship between the FTIR scans and the laser using TTL pulses. The cycle is started by collecting a spectrum before irradiation. After the data collection, the Nicolet 850 sends a signal to the counter timer, which signals a shutter to open—allowing the sample to be irradiated. After a set period of time, the shutter is closed and a data collection scan sequence is started.

The difference-frequency laser uses a Nd:YAG laser, Spectra Physics GCR-150-30, to provide 532 nm radiation and to drive the tunable dye laser.⁹ The Nd:YAG provides a 7–9 ns pulse about 30 times a second and requires 10 s to warm and produce a stable pulse. Stable operating conditions were achieved by letting the laser run continuously and using the shutter.

To follow the decay of the nonequilibrium conformations, the sample has to be left in the dark. This was achieved by blocking the FTIR beam using the “beam shuttle” mirrors of the FTIR and by blocking the laser beam with the shutter. The shortest irradiation time that can be reproducibly examined with this system is determined by the response time of the mechanical shutter and beam shuttle.

Our previous sample optics were modified to allow both the laser beam and the FTIR beam to pass through the sample simultaneously (Figure 1). The FTIR beam is conducted on a path defined using the standard Nicolet mirrors to steer the beam through the sample cell to an external InSb detector. The laser beam enters the sample chamber from another direction and is directed and focused on the sample by a combination of a 30-cm focal length spherical mirror and a flat mirror. A small IR

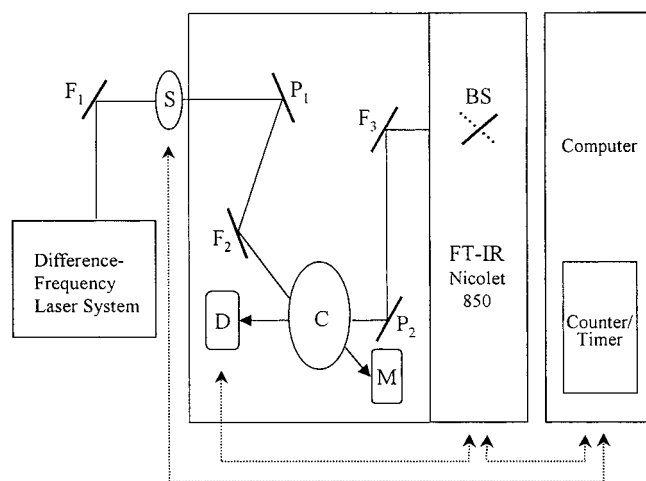


Figure 1. Optical layout. The FTIR is a Nicolet 850 with a beam shuttle, which directs the infrared beam through the cryostat C to the detector D. The cryostat contains the sample. The detector is a liquid nitrogen-cooled InSb detector. The difference frequency laser system generates an infrared beam which goes through the sample and is monitored by the Molectron, J8LP Joulemeter. The laser beam is routed through a computer-controlled shutter S. The mirrors F1, F2, and F3 are flat, the mirror P1 is a spherical mirror of 30-cm focal length, and the mirror P2 is a standard parabolic mirror from Nicolet. The beam shuttle, BS, is used as the shutter for the FTIR beam.

detector (Molectron, J8LP Joulemeter) is placed after the sample to allow aiming of the laser beam.

The sample itself is milled with mineral oil and held between two CaF_2 plates in a closed-cycle refrigerator. A mask with a hole of about 1.5 mm diameter is placed over the front plate to define the intersection of the two IR beams.

The timing diagram for the irradiation of the sample and the subsequent acquisition of the spectrum is shown in Figure 2. As already mentioned, the laser pulses were of about 7–9 ns duration with an interval between pulses of 33 ms. The total irradiation time was long (10 min) or short (10 s). The spectrum acquisition time was matched to the scan time, so, for example, the long irradiation was followed by 10 min of data collection. The moving mirror of the FTIR was driven at the relatively high speed of 11/8 cm/s and 8 scans took 10 s. For the short-time irradiation, the data was collected in 10-s intervals; each one was separated by 10 s of time in the dark. The interval was then lengthened to 1 min and finally the cycle ended with the 30-min dark period. The entire short-time cycle was repeated 60 times in order to compare with the long-time irradiation.

Equimolar quantities of nickel and ammonium sulfates were dissolved in water containing some D_2O . The solution was slowly evaporated to form crystals, which were washed with ethanol and dried. We consider samples, some containing about 5% deuterium (high concentration, HC), one containing about 1% deuterium (LC), and finally one containing an intermediate concentration of 3% (MC).

Results

In Figures 3 and 4, the infrared spectra of the HC and LC samples of the nickel Tutton salt are displayed. The spectra in 3c and 4c are the infrared absorption spectra in the O–D, N–D stretching region. Panels 3a and 4a show the difference spectra after 10 s of irradiation, while 3b and 4b show the difference spectra after 10 min of irradiation. Note the differences among the absorption scales for the various spectra. The assignment of the 10 stretching bands is shown in Table 1 together with the geometrical parameters of the hydrogen bonds as determined

by neutron diffraction at room temperature.¹⁰ The assignment uses the correlation between frequency and bond parameters established by Oxton and Knop.¹¹ The positions of the holes and anti-holes are the same in both spectra although there are obvious differences between the short- and long-irradiation time spectra.

The difference spectra for the long-irradiation times are the same as those we have obtained previously and show changes in the N–D bands only. The spectra for short-irradiation times differ and form holes/anti-holes among the O–D bands as well as among the N–D bands. We repeated the short-irradiation-time experiments, but burned each of the other three N–D bands in turn. This produced holes/anti-holes in the O–D bands as well in a pattern that is distinct for irradiation at each of the four N–D bands.

To compare the spectra in more detail, we expand the scale of the short-irradiation N–D holes and superimpose them on the long-irradiation holes in Figure 5. The holes of N–D I are very similar except for the widths. The short-irradiation holes are the same width for both deuterium concentrations. The long-irradiation holes have wider widths, and the HC width is greater than the LC width.

A third deuterium concentration sample, MC, was also investigated. Figure 7 compares the absorption spectra and the long-irradiation difference spectra. The MC spectra are intermediate between those of the LC and HC spectra. The line widths and the apparent resolution of the bands vary, as do the hole widths. Broad-band irradiation (from the FTIR source) for many hours produces similar results in the LC and HC samples (Figure 6). The absorbance of the crystals varies as expected with the HC spectrum again showing wider lines.

Irradiation moves the distribution of the X–D bands away from equilibrium. The distributions decay back to equilibrium in the dark and, of course, the holes and anti-holes decay in concert. Figure 8 shows the decay of the N–D I hole for the HC sample. Panel a shows the decay of the short-irradiation-time sample – a decay that is exponential and occurs with a time constant of 15 ± 2 min. Panel b shows the decay of the N–D I hole after the long irradiation and decays with a time constant of 110 ± 3 min, a factor of 7 slower. The O–D holes/anti-holes relax somewhat faster than the N–D hole, but these holes were so weak, we could not obtain accurate time constants for their decay.

Discussion

Previously we have studied the relaxation kinetics of ammonium cobalt Tutton salt. The relaxation process involves tunneling of the ammonium ion (NH_3D^+) among its four possible distinct orientations. The overall kinetics are the result of the various first-order rates for the various tunneling processes, and the relaxation for any given hole/anti-hole is a sum of a number of exponential decays. For the Co Tutton salt at 20 K, the approximate decay time constants are 84 and 600 min^2 . This compares well with the value of 110 min measured here for the Ni Tutton salt. We have suggested an elementary mechanism for coupling of the N–D stretch to the rotation of the ammonium ion. The N–D–O hydrogen bonds that hold the ammonium ion position in the Tutton salts are not straight. Adding energy to the N–D bond changes its length and results in a torque; see diagram in ref 3. A quantum mechanical description can be derived from the classical picture by considering the overlap factors among the various librational wave functions in the ground and excited stretch vibration states.

The result of the short-time irradiation is quite different. First, the relaxation time is only 15 min. Second, the OD bands form

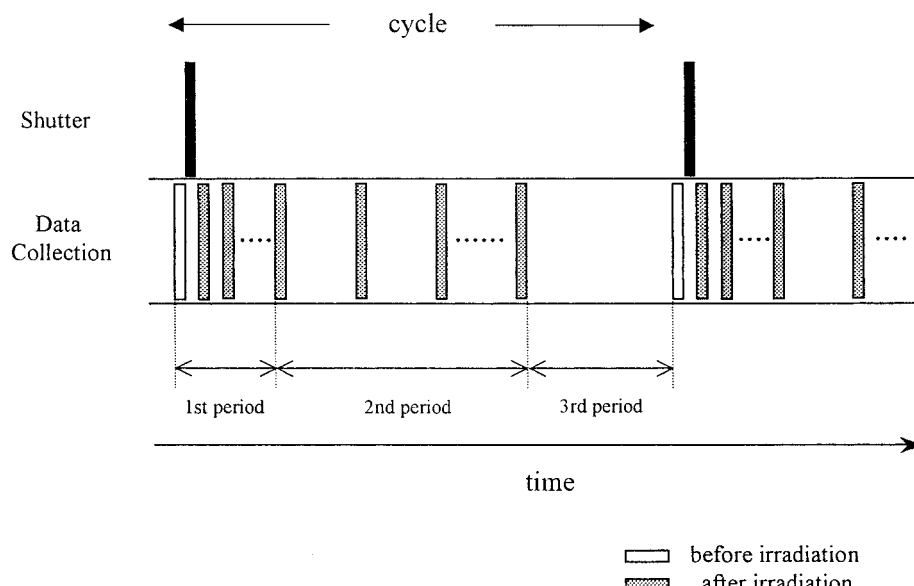


Figure 2. Timing diagram for the short-time irradiation cycle. The cycle starts with a scan before irradiation (unfilled rectangle). This is followed by irradiation (filled rectangle) and then by a series of scans (hatched rectangles). Each of these represent 10-s intervals and the first 7 scans are separated by 10-s intervals. After the seventh scan, the interval is increased to 1 min until the 30th scan. The cycle is concluded with a 30-min dark period and then repeated.

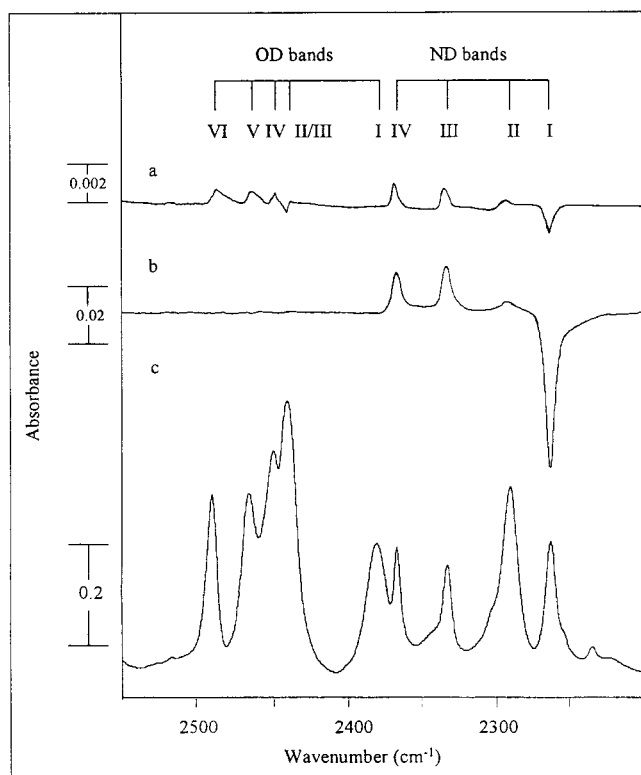


Figure 3. Infrared hole-burning spectra of ammonium nickel Tutton salt with about 5% deuterium at 20 K: (a) the difference between the spectrum after 10-s irradiation and that before; (b) the difference spectrum for 10-min irradiation; (c) the original spectrum. The laser frequency was set to the position of the ND band I. The result for one cycle of 10-s irradiation was repeated 60 times and then averaged. Note the scale differences of an order of magnitude for each panel.

holes/anti-holes, a situation not observed for the longer irradiation time nor for the cobalt salt. We have observed changes in the OD stretches in only two other situations: a mixed Co–Ni Tutton salt^{3,4} and the Cu Tutton salt.⁵ In the mixed salt, the time constant for changes in the OD stretches is much longer than for the changes in the ND stretches. For the Cu salt, the

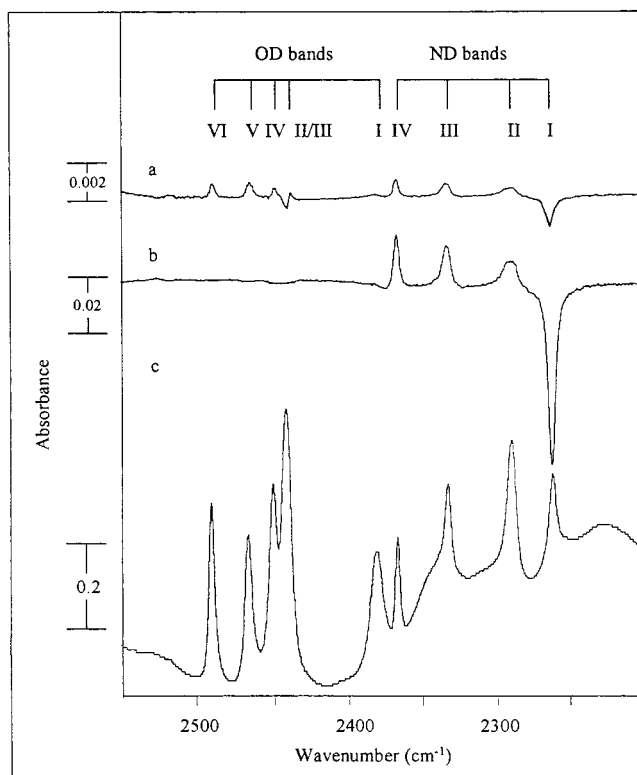


Figure 4. Infrared hole-burning spectra of ammonium nickel Tutton salt with 1% deuterium at 20 K: (a) the difference spectrum for the 10-s irradiation; (b) the difference spectrum for 10-min irradiation; (c) the original spectrum. The experimental conditions are the same as in Figure 3.

various changes have the same rates, but these are nonmonotonic. The Tutton salts thus show a range of coupled motions—motions initiated by the excitation of the N–D stretches of the ammonium ions. Note that the structure of the Tutton salts has the ammonium ion hydrogen bonded to the sulfate ions, which in turn are hydrogen bonded to the water molecules. In order for an excitation of the ammonium ion to move a water molecule, the rotation of the ammonium must rotate a sulfate

TABLE 1: Assignment of Hydrogen Bonds X–H–O in Ammonium Nickel Tutton Salt

band no.	X–O ^a	X–O ^a distance (Å)	X–H–O ^a angle (deg)	wavenumber ^b	
				HC	LC
I	N(10)–O(5)	2.854	177.1	2262.2	2262.2
II	N(10)–O(6)	2.906	162.2	2289.3	2289.1
III	N(10)–O(3)	2.956	158.4	2331.9	2331.9
IV	N(10)–O(3) ^c	2.962	163.4	2365.3	2365.8
	N(10)–O(4) ^c	3.166	130.3		
I	O(8)–O(4)	2.697	178.6	2379.5	2379.7
II	O(9)–O(3) ^d	2.709	170.6	2440.0	2440.0
III	O(8)–O(6) ^d	2.758	174.5		
IV	O(9)–O(5)	2.765	168.7	2448.9	2448.9
V	O(7)–O(5)	2.782	170.6	2465.4	2465.4
VI	O(7)–O(6)	2.828	169.9	2490.3	2490.3

^a From ref 10 at room temperature. ^b From this work at 20 K. ^c Bifurcated hydrogen bond. ^d OD bands II and III are difficult to distinguish in the infrared spectrum.

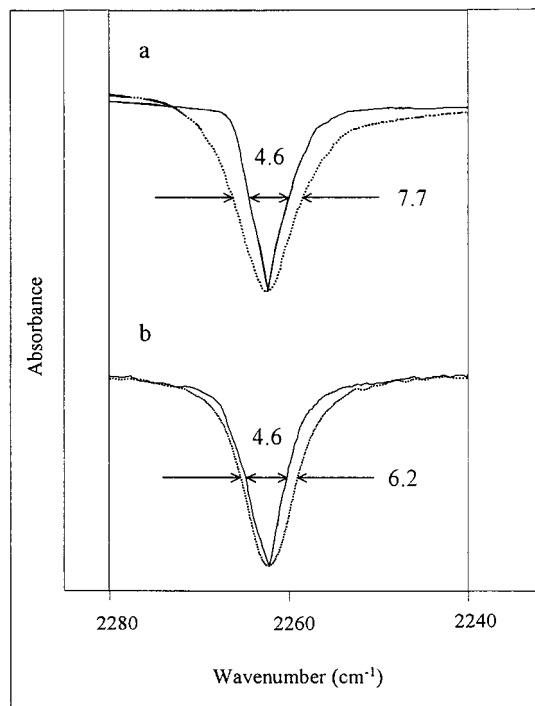


Figure 5. Comparison between N–D I hole with 10-s irradiation time (solid line) and that with 10-min irradiation time (dotted line): (a) the hole widths of the HC sample; (b) the hole widths of LC. The scales for the solid lines in (a) and (b) are expanded by factors of 33 and 40, respectively.

ion, which in turn moves a water molecule. Additional evidence for coupling of motions comes from detailed analysis of the thermal atomic displacements of the potassium–ruthenium Tutton salt X-ray diffraction patterns.^{12,13} In most cases the thermal atomic displacements fit the predictions of the internal force field plus a term for the translation–rotation of the molecule as a whole. However, the potassium–ruthenium Tutton salt does not follow the general rule. Instead, the Ru–O–H stretching motion must be coupled to the translation of the Ru–(H₂O)₆⁺⁺ ion to fit the data.^{13,14}

The initial observation that the hole burning is different on the two different times of burning shows that there are at least two sets of relaxations for the Ni salt. The faster one equilibrates on the time scale of the longer irradiation (10 min). Consequently, the holes/anti-holes stay small on the scale of the holes produced in the N–D bands on long irradiation. The short-time relaxation is much more complex involving both O–D and

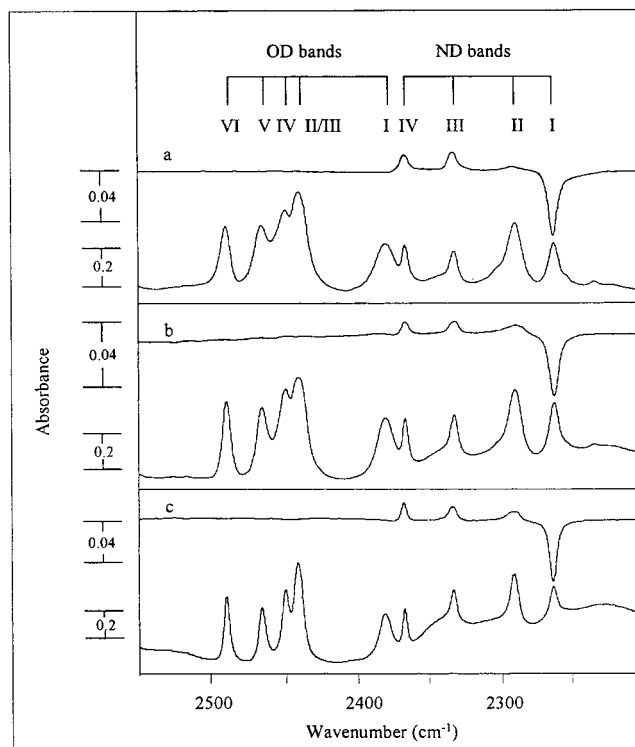


Figure 6. Comparison of the infrared spectra of the nickel Tutton salt containing different amounts of deuterium. For each set, the upper spectrum is the difference spectrum with 10-min irradiation and the lower is the original spectrum: (a) HC; (b) MC; (c) LC. The laser frequency was set to the position of N–D I. The scale of the upper and the lower spectra differs by 1 order of magnitude in each set.

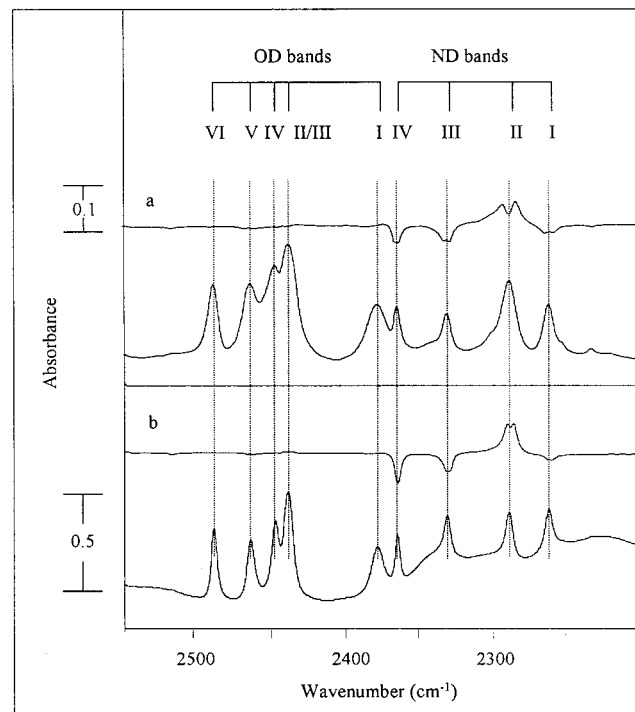


Figure 7. The difference spectra of ammonium nickel Tutton salt after broad-band irradiation overnight: (a) HC: the difference spectrum and the original spectrum; (b) LC: the difference spectrum and the original spectrum.

N–D conformations and bonds, while the slower set of processes involves only the reorientation of the NH₃D⁺ ions.

Burning the N–D I band excites both sets of processes. Some indication that there are indeed two sets is shown by the width

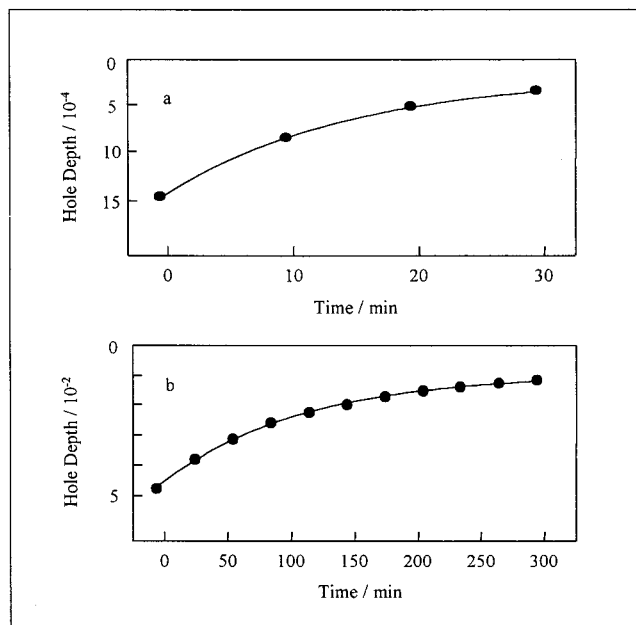


Figure 8. Recovery of holes occurring with different irradiation times at N–D band I of the HC in the dark: (a) the recovery of hole with 10-s irradiation; (b) the recovery of hole with 10-min irradiation. The solid lines are single-exponential fits: (a) $\tau = (15 \pm 2)$ min and (b) $\tau = (110 \pm 3)$ min.

of the holes. As Figure 5 shows, the holes for the HC sample and the LC sample are the same on short irradiation. The long irradiation in contrast yields holes that are wider and depend on the deuterium concentration. Thus the longer irradiation must excite a wider range of N–D sites (either directly or by spectral diffusion), and these additional sites relax more slowly. A possibility is that the slower relaxing sites come from those N–D sites that interact with one another.

It is well-known that, especially in disordered systems such as a glass, relaxation of spectral holes can occur over an enormous range of time scales.¹⁵ This range arises because of the intrinsic range of environments and times for motions that lead to spectral diffusion. In our system, which is nominally that of well-ordered crystallites, we have demonstrated changes of conformation. These changes involve rotation of deuterium-containing moieties (NH_3D^+ and HOD) among well-defined crystallographic positions. By scanning these motions on two different time scales that differ by a factor of 60, we have shown that there are sets of conformational kinetics that differ by similar factors. The inhomogeneity of the X–D vibrational bands also shows up as the deuterium-dependent widths seen on the longer irradiation.

It has been found that many hydrides do not obey the simple rule for a homogeneous band that the hole width (for a small hole) should be half the width of the corresponding absorption band.^{16,17} Our investigation shows at least one possible mechanism for these anomalies: there are multiple spectral diffusion/reaction mechanisms that occur on the time scale of the laser irradiation.

For the Tutton salts we are able to identify the conformational changes that occur on this time scale. However, the differences among the different Tutton salts remain largely unknown. Although the salts all form isomorphous crystals, relatively small perturbations make a substantial difference to the structure. An extreme example is the ammonium copper Tutton salt which can exist in more than one crystal form. Although the ammonium cobalt and the ammonium nickel salts are very close in structure, the mixed crystals show slow changes on hole burning that the neat crystals do not. These unique changes must be due to strain in the mixed crystal. Here we show that the neat nickel salt shows rapid changes. We do not know whether the other Tutton salts do likewise.

Acknowledgment. We thank Christopher A. Endicott and Hung-Wen Li for their help and are pleased to acknowledge support by the National Science Foundation, Grant CHE-98-15945.

References and Notes

- (1) Montgomery, H.; Lingafelter, E. C. *Acta Crystallogr.* **1964**, *17*, 1478.
- (2) Trapani, A. P.; Strauss, H. L. *J. Am. Chem. Soc.* **1989**, *111*, 910.
- (3) Strauss, H. L. *Acc. Chem. Res.* **1997**, *30*, 37.
- (4) Fei, S.; Strauss, H. L. *J. Phys. Chem.* **1995**, *99*, 2256.
- (5) Fei, S.; Strauss, H. L. *J. Phys. Chem.* **1996**, *100*, 3414.
- (6) Chen, Z.; Fei, S.; Strauss, H. L. *J. Am. Chem. Soc.* **1998**, *120*, 8789.
- (7) Simmons, C. J.; Hitchman, M. A.; Stratemeier, H.; Schultz, A. J. *J. Am. Chem. Soc.* **1993**, *115*, 11304.
- (8) Dunn, T. M.; McClure, D. S.; Pearson, R. G. *Crystal Field Theory*; Harper & Row: New York, 1965.
- (9) Kung, A. H.; Fei, S.; Strauss, H. L. *Appl. Spectrosc.* **1996**, *50*, 790.
- (10) Maslen, E. N.; Ridout, S. C.; Watson, K. J.; Moore, F. H. *Acta Crystallogr.* **1988**, *C44*, 412.
- (11) Oxtou, L. A.; Knop, O. *J. Mol. Struct.* **1978**, *49*, 309.
- (12) Hummel, W.; Raselli, A.; Burgi, H. B. *Acta Crystallogr.* **1990**, *B46*, 683.
- (13) Burgi, H. B. *Annu. Rev. Phys. Chem.* **2000**, *51*, 275.
- (14) Burgi, H. B.; Raselli, A. *Struct. Chem.* **1993**, *4*, 23.
- (15) Littau, K. A.; Bai, Y. S.; Fayer, M. D. *J. Chem. Phys.* **1990**, *92*, 4145.
- (16) Mungan, C. E.; Happek, U.; McWhirter, J. T.; Sievers, A. J. *J. Chem. Phys.* **1997**, *107*, 2215.
- (17) Chen, Z.; Strauss, H. L. *J. Chem. Phys.* **1998**, *108*, 5522.